Physics of the Earth and Planetary Interiors 187 (2011) 66–75

Contents lists available at ScienceDirect

Physics of the Earth and Planetary Interiors

journal homepage: www.elsevier.com/locate/pepi

New $^{40}Ar/^{39}Ar$ dating results from the Shanwang Basin, eastern China: Constraints on the age of the Shanwang Formation and associated biota

Huaiyu He [a,*], Chenglong Deng [b], Yongxin Pan [a], Tao Deng [c], Zhaohua Luo [d], Jimin Sun [b], Rixiang Zhu [b]

[a] Key Laboratory of the Earth's Deep Interior, Institute of Geology and Geophysics, Chinese Academy of Sciences, Beijing 100029, China
[b] State Key Laboratory of Lithospheric Evolution, Institute of Geology and Geophysics, Chinese Academy of Sciences, Beijing 100029, China
[c] Institute of Vertebrate Paleontology and Paleoanthropology, Chinese Academy of Sciences, Beijing 100044, China
[d] China University of Geosciences, Beijing 100083, China

ARTICLE INFO

Article history:
Available online 27 May 2011
Edited by Keke Zhang

Keywords:
$^{40}Ar/^{39}Ar$ dating
Geochronology
Shanwang Formation
Shanwang biota
Miocene

ABSTRACT

The fluvio-lacustrine sequence of the Shanwang Basin, eastern China, preserves a rich and important terrestrial fossil fauna and flora; the exceptional preservation of these fossils reveals the dynamics of ancient mammalian ecosystems and plant biology. However, the timing of this sedimentary sequence has been the subject of debate for decades. Here we contribute to this debate by presenting the detailed results of $^{40}Ar/^{39}Ar$ analysis of the basalts above, below, and within the Shanwang Formation. These dates place stringent constraints on the age of Shanwang Formation and associated biota. $^{40}Ar/^{39}Ar$ ages obtained from basalts of the Niushan and Yaoshan Formations, which underlie and overlie the Shanwang Formation, are 21.0 ± 2.5 Ma (2σ, full external error) and 17.3 ± 1.5 Ma (2σ, full external error), respectively. The $^{40}Ar/^{39}Ar$ age of the basalt in the Shanwang Formation is 17–18 Ma. Given the age constraints of the basalts of the Yaoshan and Shanwang Formations, the age of the Shanwang biota is estimated to be ca. 17 Ma, late Burdigalian of the Early Miocene, indicating that the deposition of this fauna coincided with the onset of the mid-Miocene Climatic Optimum. The results provide new age constraints on the Shanwang mammal fauna, and independently support interpretations that this fauna can be assigned to chronozone MN4, and correlated with middle Orleanian of the European Land Mammal Age, and to late Hemingfordian of the North American Land Mammal Age. Biological diversity of the Shanwang Formation could reflect the global-scale mid-Miocene Climatic Optimum.

© 2011 Elsevier B.V. All rights reserved.

1. Introduction

The Shanwang Basin in eastern China is filled with lacustrine and fluvial deposits, and volcanic and volcaniclastic rocks. The sedimentary sequence has been named the Shanwang Series (Young, 1936; Young and Tchang, 1936) and the Shanwang Formation (Sun, 1961; Yan et al., 1983). The fossils from this formation, which comprise the Shanwang biota, are exceptionally well-preserved, and the unit is considered a *Konservat-Lagerstätte* (Yang and Yang, 1994). Fossils are mainly excavated from diatomaceous lacustrine shales within the Shanwang Formation; these shales have revealed and incredibly rich biota with over five hundred species currently recognized, including fungi, diatoms, vascular plants, insects, ostracodes, fish, amphibians, reptiles, birds, and mammals (Young and Tchang, 1936; Skvortzov, 1937; Teilhard De Chardin, 1939; Yan et al., 1983; Qiu and Qiu, 1995; Liu et al., 2002; Deng et al., 2003). Since the 1930s, paleontologists, paleobotanists, paleoclimatologists, and geochronologists have been attracted to the basin because of the high-quality preservation and exceptional richness of its fossil fauna and flora (e.g., Young, 1936, 1937; Yan et al., 1983; Yang and Yang, 1994; Sun et al., 2002; Liang et al., 2003; Strömberg et al., 2007). The intense research that resulted has contributed significantly to our understanding of the paleoclimate, paleoecology and biochronology of the Miocene in eastern China (Li et al., 1984; Qiu and Qiu, 1995; Yang, 2000; Sun et al., 2002; Deng et al., 2003; Sun and Wang, 2005; Deng, 2006; Strömberg et al., 2007; Yang et al., 2007; Li et al., 2010).

Li et al. (1984) used the Shanwang fauna to define one of the Eastern Asian Land Mammal Ages of the Neogene, the Shanwangian Age, a term that has been widely adopted by paleontologists (e.g., Qiu and Qiu, 1995; Tong et al., 1995; Qiu et al., 1999; Deng, 2006; Deng et al., 2003). Unfortunately, the lack of accurate radioisotopic dates for the Shanwang Formation and associated Shanwang fauna has prevented accurate correlation of the Shanwangian East Asian Land Mammal Age with the European Land Mammal Ages or the North American Land Mammal Ages, both of which are well-calibrated and widely-used biochronological timescales (Gradstein et al., 2004; Ogg et al., 2008).

The Shanwang flora contains a plethora of evidence regarding terrestrial ecosystems during the Early or Middle Miocene (Sun et al., 2002; Liang et al., 2003; Wang, 2006; Strömberg

* Corresponding author. Tel.: +86 10 8299 8414.
E-mail addresses: huaiyuhe@mail.iggcas.ac.cn, huaiyuhe@yahoo.com (H. He).

0031-9201/$ - see front matter © 2011 Elsevier B.V. All rights reserved.
doi:10.1016/j.pepi.2011.05.002

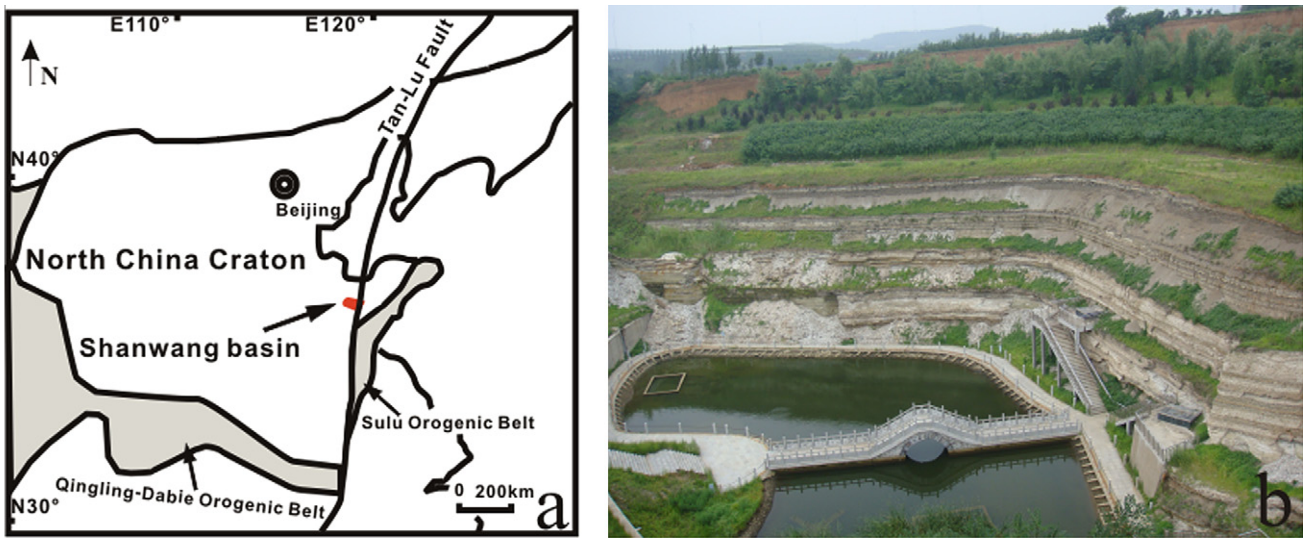

Fig. 1. (a) Schematic map showing the Shanwang Basin and its adjacent regions. (b) A close view of the fossil-bearing diatomaceous shales in the Shanwang Basin.

et al., 2007). The lack of precise age constraints on the timing of the deposition of the Shanwang Formation and associated flora hinders our understanding of ecological processes and their relationship with regional and global ecological processes during a critical period. Therefore, systematic dating of the basalts above, below, and within the Shanwang Formation is needed in order to precisely constrain the age of the Shanwang Formation.

Here we address this issue by presenting the results of a detailed $^{40}Ar/^{39}Ar$ analysis of the basalts in the Shanwang Basin. To be concordant with the Geologic Time Scale 2004 (Gradstein et al., 2004), all $^{40}Ar/^{39}Ar$ ages presented herein are calculated to be consistent with an age of 28.34 ± 0.28 Ma for the sanidine (TCR-sanidine standard) from the Taylor Creek Rhyolite (Renne et al., 1998). The uncertainties of the ages were reported as two sigma full external error, where full external error combines the

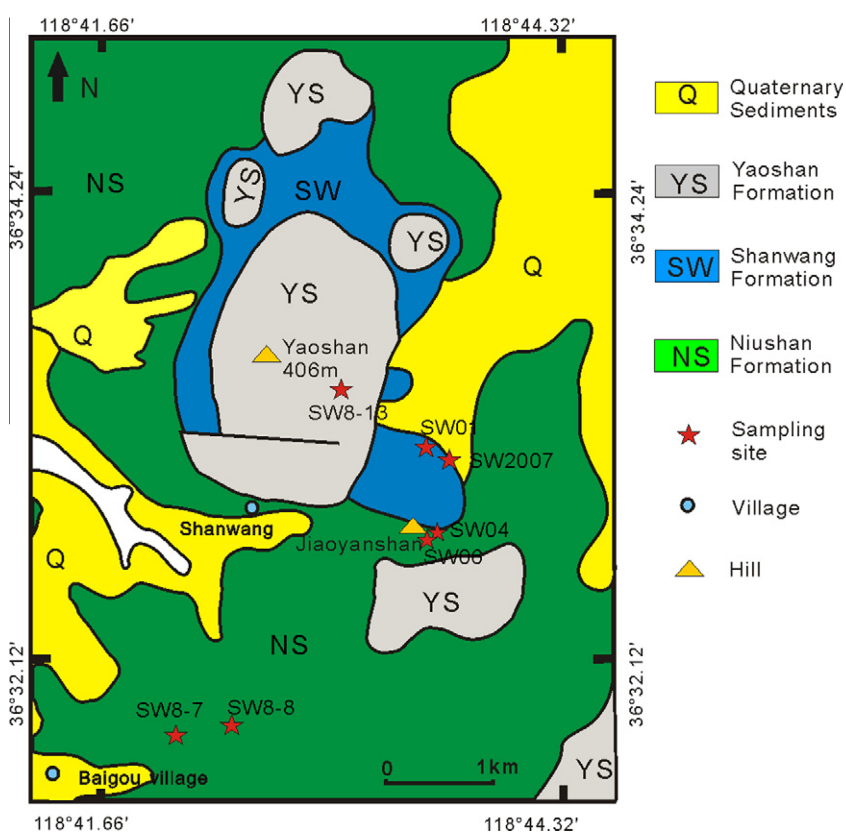

Fig. 2. Geological map showing the distribution of strata in the Shanwang Basin (modified from SPBGMR, 1991). The strata are divided into three formations, listed in ascending order: the Niushan Formation, the Shanwang Formation and the Yaoshan Formation. The Niushan Formation mainly consists of tholeiite basalt, the Shanwang Formation, mainly of lacustrine sediments and interbedded basalts, and the Yaoshan Formation, mainly of alkalic basalts.

analytical error, the error on the *J*-value and the systematic error on the total decay constant λ.

2. Geological setting and sampling

The Shanwang Basin is located in the eastern part of the North China Craton and the middle part of the Tan-Lu fault zone (Fig. 1a). The Miocene strata in this basin consist of three lithologic formations, from bottom to top, the Niushan, Shanwang and Yaoshan Formations (Fig. 2). Olivine tholeiite magma activity began during the early Neogene; the products of these eruptions blanketed the area and formed the Niushan Formation. Later, lacustrine and fluvio-lacustrine sediments with inter-bedded basalts filled the topographic lows of the earlier lava sheets, forming the Shanwang Formation. The latest alkalic olivine basalt of the Yaoshan Formation breaks out through the Niushan and Shanwang Formations, capping the Miocene sequence in the studied area (Fig. 2) (SPBGMR, 1991; Li, 1991; Luo et al., 1992; Yang, 2000; Guo et al., 2007).

Overlying Precambrian metamorphic rocks, the Niushan Formation is mainly comprised of olivine tholeiite basalts with some basanite and alkaline basalts, derived from the primitive alkalic olivine basaltic magma by fractional crystallization (Xu and Qiu, 1991). These basalts are porphyritic, with olivine and plagioclase phenocrysts, and a matrix consisting of glassy material, olivine, plagioclase and some clinopyroxene. Conformably overlying the Niushan Formation, the Shanwang Formation consists of, from the top to bottom, yellowish brown basaltic sandy-conglomerates, inter-bedded basalts, gray or yellow shales with dark brown coal lenses, gray diatomaceous shale with black phosphate nodules and carbonaceous layers, brownish yellow tuffaceous sandy-conglomerates and breccias. The Yaoshan Formation mainly consists of fluvial conglomerates and alkaline basalts.

The Jiaoyanshan–Yaoshan section (Fig. 2) preserves the complete stratigraphic sequence of the Shanwang Basin. From Jiaoyanshan to Yaoshan, five lava flows were sampled for radioisotopic dating (Fig. 3). Samples SW04 and SW06, from the base of the Jiaoyanshan Hill, are from the Niushan Formation. Two samples (SW2007 and SW01) were collected from the vesicular basalt just below the diatomaceous sediments of the Shanwang Formation. Sample SW8-13, collected from a lava flow on the slope of Yaoshan Hill, is from the Yaoshan Formation (Fig. 2).

The Baigou village section, located approximately two kilometers southeast of the Jiaoyanshan–Yaoshan section, preserves more than ten basalt lava flows within the Niushan Formation. Two samples were taken from this section, sample SW8-7 from the upper section and sample SW8-8 from the lower section.

3. $^{40}Ar/^{39}Ar$ analytical methods

The basalt samples were crushed and sieved at 40–80 (380–200 μm) mesh fractions. After all visible crystals and impurities were removed by hand under a binocular microscope, the fresh matrix was washed with acetone in an ultra-sonic bath for 20 min. To remove possible alteration, the matrix sample was washed with 5% HNO_3 in an ultra-sonic bath for 20 min. The grains were then rinsed with distilled water and dried. Approximately 3–4 mg of sample was wrapped into a 5 mm in diameter and 1 mm thick disc by Al foil, stacked in vacuum sealed quartz vials. TCR-sanidine standards, optical CaF_2 and K-glass monitors, were stacked between the samples. The vials were shielded with cadmium foil (0.5 mm thick) and irradiated in position H8 of the 49-2 reactor, Beijing, China, for 30 h. To minimize the effects of vertical gradient, we carefully controlled the vertical position of the unknown samples and the monitors, and used at least four monitors within a vertical distance of less than 2.5 cm. For horizontal gradient, we packed the samples in 5 mm Al disk and rotated the cans during the irradiation.

$^{40}Ar/^{39}Ar$ step-heating analyses by furnace were performed on a MM5400 mass spectrometer operating in static mode. The total system blanks (1000 °C, 20 min) were in the range of $(4.9–5.8) \times 10^{-16}$ moles for mass 40, $(0.9–1.4) \times 10^{-18}$ moles for mass 39, $(8.7–9.2) \times 10^{-19}$ moles for mass 37, and $(1.8–2.1) \times 10^{-18}$ moles for mass 36. Mass discrimination (0.009934–0.009958 per atomic mass unit) was monitored by analysis of $^{40}Ar/^{36}Ar$ air pipette aliquots each day. Ca, K correction factors were calculated from the CaF_2 and K-glass monitors: $(^{40}Ar/^{39}Ar)_K = 8.8 \times 10^{-4}$, $(^{39}Ar/^{37}Ar)_{Ca} = 7.24 \times 10^{-4}$, $(^{36}Ar/^{37}Ar)_{Ca} = 2.39 \times 10^{-4}$. The data were corrected for system blanks, mass discriminations, interfering Ca, K derived argon isotopes, and the decay of ^{37}Ar since the time of the irradiation. The decay constant used throughout the calculations is $\lambda = (5.543 \pm 0.010) \times 10^{-10} \cdot a^{-1}$, as recommended by Steiger and Jaeger (1977). The uncertainty of *J*-value (0.2–0.5% in this work) is one standard deviation of mean; this was propagated into the final plateau and isochron ages, and contributed about 40% to the total uncertainty in these age determinations. The uncertainties of the ages were reported as internal error combines the analytical error and the error on the standard, details of the step-heating procedures were outlined in He et al. (2004). The plateau and isochron ages were calculated using ArArCALC (Koppers, 2002). A plateau age from an age spectrum is assigned when at least three successive incremental heating steps yield consistent apparent ages

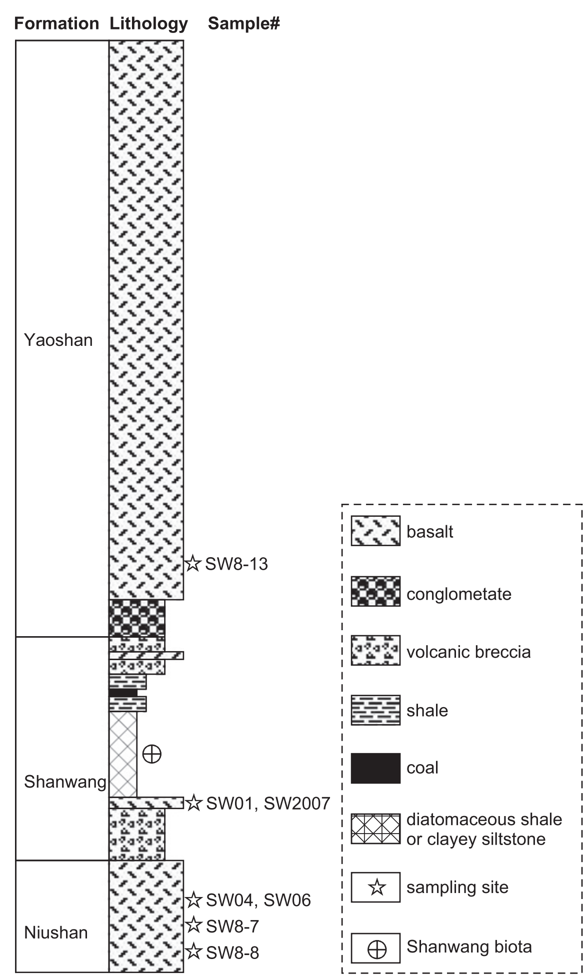

Fig. 3. Composite stratigraphic sequence of the Shanwang Basin. Note that the thickness for each bed is relative.

Table 1
$^{40}Ar/^{39}Ar$ step-heating data for samples from the Shanwang Basin.

Temp (°C)	$^{39}Ar/^{40}Ar$ ± 1s.d. (10^{-2})	$^{36}Ar/^{40}Ar$ ± 1s.d. (10^{-4})	$^{37}Ar/^{39}Ar$	^{39}Ar cum(%)	$^{40}Ar^*$ (%)	$^{40}Ar^*/^{39}Ar$	Apparent age ± 2s.d. (Ma)
SW04, Niushan Formation J = 0.005244 ± 0.000010							
800	27.14 ± 0.07	13.71 ± 0.16	1.20	7.33	59.48	2.19	20.67 ± 0.34
850	7.49 ± 0.02	29.32 ± 0.24	1.02	15.57	13.36	1.78	16.84 ± 1.77
890	16.86 ± 0.04	22.22 ± 0.21	0.96	7.51	34.33	2.04	19.21 ± 0.70
930	29.86 ± 0.09	12.60 ± 0.15	1.54	5.73	62.76	2.10	19.83 ± 0.31
970	26.05 ± 0.08	14.79 ± 0.23	2.19	5.12	56.30	2.16	20.38 ± 0.52
1020	26.25 ± 0.06	15.35 ± 0.19	2.06	6.71	54.63	2.08	19.63 ± 0.41
1070	22.03 ± 0.08	18.75 ± 0.25	2.33	5.36	44.60	2.02	19.10 ± 0.66
1130	26.06 ± 0.07	13.61 ± 0.50	3.47	6.88	59.79	2.29	21.62 ± 1.06
1200	36.78 ± 0.13	5.51 ± 0.13	6.03	32.98	83.71	2.28	21.46 ± 0.26
1270	21.25 ± 0.07	0.03 ± 0.49	55.53	3.88	100.07	4.71	44.12 ± 1.28
1330	11.01 ± 0.03	15.75 ± 0.36	54.81	2.33	53.46	4.85	45.45 ± 1.83
1400	20.00 ± 0.17	1.92 ± 0.73	62.86	0.60	105.66	5.28	49.42 ± 2.13
SW06, Niushan Formation J = 0.005266 ± 0.000010							
800	8.20 ± 0.06	28.58 ± 0.25	1.88	11.95	15.54	1.90	17.96 ± 1.75
860	1.64 ± 0.02	33.24 ± 0.27	1.74	12.15	1.79	1.09	10.35 ± 9.21
900	15.26 ± 0.04	22.41 ± 0.21	1.36	4.69	33.78	2.21	20.96 ± 0.77
940	21.83 ± 0.08	18.07 ± 0.26	1.63	5.81	46.59	2.13	20.21 ± 0.70
980	26.25 ± 0.08	14.94 ± 0.18	1.82	8.29	55.85	2.13	20.15 ± 0.41
1020	29.21 ± 0.12	12.17 ± 0.21	2.02	7.40	64.02	2.19	20.75 ± 0.45
1070	24.13 ± 0.09	16.19 ± 0.20	1.93	8.08	52.15	2.16	20.46 ± 0.51
1130	21.43 ± 0.06	18.01 ± 0.29	3.32	7.80	46.79	2.18	20.67 ± 0.78
1190	35.04 ± 0.09	5.52 ± 0.17	8.84	12.70	83.68	2.39	22.60 ± 0.30
1260	31.87 ± 0.07	7.43 ± 0.36	37.98	19.00	121.93	3.83	36.07 ± 0.65
1320	18.88 ± 0.20	22.01 ± 1.26	123.20	1.61	165.04	8.74	81.40 ± 3.89
1400	8.98 ± 0.11	8.33 ± 0.88	89.38	0.51	75.37	8.39	78.18 ± 5.71
SW8-7, Niushan Formation J = 0.004836 ± 0.000024							
890	0.24 ± 0.01	33.09 ± 0.43	0.31	2.62	2.23	9.32	79.70 ± 88.61
1010	0.56 ± 0.00	33.05 ± 0.40	0.72	19.06	2.34	4.22	36.50 ± 36.63
1050	0.93 ± 0.00	33.04 ± 0.40	0.76	12.99	2.37	2.56	22.21 ± 21.94
1090	0.87 ± 0.00	32.92 ± 0.40	0.85	8.70	2.72	3.11	27.03 ± 23.37
1130	1.21 ± 0.01	33.00 ± 0.40	1.98	6.36	2.48	2.04	17.78 ± 16.91
1180	2.68 ± 0.01	32.14 ± 0.41	3.92	8.28	5.02	1.87	16.27 ± 7.88
1230	3.27 ± 0.01	30.75 ± 0.38	8.81	26.25	9.14	2.79	24.26 ± 5.96
1270	3.26 ± 0.01	32.03 ± 0.43	23.09	8.83	5.36	1.64	14.32 ± 6.74
1340	2.43 ± 0.02	31.50 ± 0.45	40.73	3.32	6.91	2.84	24.69 ± 9.38
1450	3.19 ± 0.03	29.97 ± 0.42	24.09	3.60	11.44	3.59	31.11 ± 6.75
SW8-8, Niushan Formation J = 0.0048902 ± 0.00245							
890	0.27 ± 0.00	33.69 ± 0.42	0.28	2.74	0.45	1.68	14.77 ± 80.74
940	0.34 ± 0.01	32.92 ± 0.47	0.37	5.31	2.71	8.09	70.14 ± 70.52
980	0.45 ± 0.00	32.21 ± 0.38	0.68	14.38	4.81	10.74	92.56 ± 42.73
1010	0.87 ± 0.00	33.21 ± 0.40	0.82	13.29	1.87	2.15	18.93 ± 23.87
1040	1.29 ± 0.00	32.59 ± 0.39	0.85	9.77	3.71	2.87	25.17 ± 15.61
1070	1.65 ± 0.01	32.31 ± 0.39	0.77	8.06	4.52	2.74	24.07 ± 12.32
1100	1.41 ± 0.01	32.48 ± 0.40	0.88	5.44	4.01	2.85	25.04 ± 14.60
1140	1.26 ± 0.01	32.71 ± 0.41	1.35	3.34	3.35	2.64	23.24 ± 16.60
1180	2.56 ± 0.02	31.96 ± 0.41	2.86	2.96	5.55	2.16	19.04 ± 8.36
1230	4.67 ± 0.02	29.99 ± 0.38	5.90	23.96	11.37	2.44	21.43 ± 4.20
1270	4.22 ± 0.02	30.49 ± 0.40	22.81	6.73	9.90	2.35	20.64 ± 4.94
1330	3.28 ± 0.02	31.40 ± 0.45	36.82	2.29	7.22	2.20	19.35 ± 7.04
1450	2.53 ± 0.03	31.82 ± 0.45	39.60	1.73	5.98	2.37	20.79 ± 9.23
SW01, Shanwang Formation J = 0.005225 ± 0.000010							
780	6.64 ± 0.04	29.05 ± 0.27	1.38	15.63	14.15	2.13	20.03 ± 2.32
830	6.54 ± 0.02	29.22 ± 0.24	1.53	16.18	13.64	2.09	19.60 ± 2.05
880	3.92 ± 0.02	31.44 ± 0.27	2.03	14.57	7.10	1.81	17.05 ± 3.77
920	3.42 ± 0.03	31.86 ± 0.26	1.68	14.29	5.86	1.71	16.09 ± 4.26
960	5.02 ± 0.05	31.00 ± 0.27	1.28	10.02	8.41	1.68	15.77 ± 3.02
1000	10.35 ± 0.14	28.07 ± 0.29	1.21	8.78	17.04	1.65	15.49 ± 1.64
1050	10.77 ± 0.03	25.81 ± 0.29	1.88	3.37	23.72	2.20	20.69 ± 1.50
1100	9.36 ± 0.03	26.36 ± 0.23	3.26	3.52	22.10	2.36	22.16 ± 1.38
1160	8.31 ± 0.02	26.42 ± 0.25	7.60	3.72	21.93	2.64	24.78 ± 1.66
1300	12.45 ± 0.04	10.63 ± 0.23	36.94	7.19	68.58	5.51	51.31 ± 1.06
1450	12.28 ± 0.06	10.20 ± 0.39	34.17	2.74	69.86	5.69	52.98 ± 1.81
SW2007, Shanwang Formation J = 0.003500 ± 0.000009							
780	4.97 ± 0.09	31.40 ± 0.81	0.50	7.99	7.21	1.45	9.14 ± 6.20
840	17.17 ± 0.45	21.45 ± 0.91	0.46	9.74	36.61	2.13	13.45 ± 2.43
890	11.16 ± 0.12	25.67 ± 0.57	0.47	15.09	24.15	2.16	13.65 ± 1.99
940	22.99 ± 0.18	13.10 ± 0.30	0.46	20.34	61.27	2.67	16.79 ± 0.58
980	24.27 ± 0.16	10.23 ± 0.23	0.51	18.16	69.76	2.87	18.11 ± 0.44
1030	21.45 ± 0.13	13.93 ± 0.36	0.52	8.30	58.83	2.74	17.28 ± 0.68
1110	18.77 ± 0.10	15.55 ± 0.31	0.95	14.57	54.03	2.88	18.13 ± 0.64
1150	19.17 ± 0.13	8.52 ± 0.26	7.46	4.10	74.83	3.90	24.54 ± 0.60

(*continued on next page*)

Table 1 (*continued*)

Temp (°C)	$^{39}Ar/^{40}Ar$ ± 1s.d. (10^{-2})	$^{36}Ar/^{40}Ar$ ± 1s.d. (10^{-4})	$^{37}Ar/^{39}Ar$	^{39}Ar cum(%)	$^{40}Ar^*$ (%)	$^{40}Ar^*/^{39}Ar$	Apparent age ± 2s.d. (Ma)
1200	2.65 ± 0.03	2.84 ± 0.15	44.09	0.51	91.62	34.57	206.53 ± 4.63
1260	0.76 ± 0.01	0.54 ± 0.03	22.04	0.34	98.40	130.02	678.22 ± 10.79
1320	0.65 ± 0.01	0.45 ± 0.06	21.18	0.16	98.66	150.63	765.70 ± 22.56
1380	9.12 ± 0.16	3.81 ± 0.25	3.54	0.33	88.73	9.73	60.53 ± 2.54
1450	0.88 ± 0.01	0.79 ± 0.04	7.33	0.36	97.67	111.04	593.70 ± 11.11
SW8-13, Yaoshan Formation J = 0.004929 ± 0.000025							
890	0.60 ± 0.00	33.38 ± 0.40	0.27	6.43	1.37	2.29	20.32 ± 35.27
940	1.89 ± 0.01	32.00 ± 0.39	0.34	8.65	5.44	2.88	25.49 ± 10.61
980	2.51 ± 0.01	31.55 ± 0.39	0.38	13.90	6.77	2.70	23.88 ± 8.16
1010	5.53 ± 0.02	30.32 ± 0.38	0.49	10.79	10.42	1.88	16.71 ± 3.61
1040	7.17 ± 0.03	29.14 ± 0.36	0.60	8.42	13.90	1.94	17.19 ± 2.61
1070	6.83 ± 0.03	29.47 ± 0.38	0.69	7.21	12.92	1.89	16.77 ± 2.95
1110	5.90 ± 0.04	29.92 ± 0.36	0.72	7.46	11.59	1.96	17.41 ± 3.22
1150	6.34 ± 0.03	29.57 ± 0.39	0.69	8.42	12.62	1.99	17.66 ± 3.20
1190	10.03 ± 0.06	26.80 ± 0.38	0.95	9.37	20.81	2.07	18.40 ± 2.00
1230	11.84 ± 0.07	25.72 ± 0.35	3.11	8.79	24.00	2.03	17.97 ± 1.57
1270	12.12 ± 0.07	25.56 ± 0.37	9.70	7.16	24.48	2.02	17.90 ± 1.60
1330	7.01 ± 0.05	28.35 ± 0.52	51.32	2.15	16.22	2.31	20.49 ± 3.93
1450	5.18 ± 0.06	26.97 ± 0.80	78.07	1.04	20.31	3.92	34.63 ± 8.04
1500	3.66 ± 0.30	20.58 ± 0.85	6.76	0.21	39.17	10.71	93.02 ± 18.92

within error limits, and covers a minimum of 50% of the total released ^{39}Ar. When these criteria are not met, a near plateau age is calculated. The results of the $^{40}Ar/^{39}Ar$ experiments are listed in Table 1 and plotted as age spectrum and isotope correlation diagrams in Figs. 4–6.

4. Results

4.1. The Niushan Formation

Sample SW04 gives a strongly discordant age spectrum (Fig. 4a), yet a large percentage of the gas (70%, seven consecutive steps) suggests a near plateau age of about 20 Ma. These seven steps yield an inverse isochron age of about 21 Ma (Fig. 4b). We regard the near plateau age of 20 Ma as approximation for the time since lava SW04 erupted.

Sample SW06 also gives a discordant age spectrum (Fig. 4c). Despite this, six consecutive steps, which account for 42.1% of the total ^{39}Ar released, suggests a near plateau age of 21 Ma (Fig. 4c). These seven steps yield an inverse isochron age of about 20 Ma (Fig. 4d). We regard the near plateau age of 21 Ma as approximation for the time since lava SW06 erupted.

Sample SW8-7 yields a discordant age spectrum with very large error bar due to low amounts of radiogenic ^{40}Ar, consistent with its low K content and vesicular texture (Fig. 4e). Seven consecutive steps, which account for 74.7% of the total ^{39}Ar released, suggests a plateau age about 20 Ma (Fig. 4e). These seven steps yield an inverse isochron age of about 19 Ma (Fig. 4f). We regard the near plateau age of 20 Ma as approximation for the time since lava SW8-7 erupted.

Sample SW8-8 gives a concordant age spectrum (Fig. 4g). Ten consecutive steps which account for 77.6% of the total ^{39}Ar released, define a plateau age of 21.0 ± 2.5 Ma (MSWD = 0.2) (Fig. 4g). An inverse isochron age of 19.9 ± 4.9 Ma (MSWD = 0.2) (Fig. 4h), calculated from these plateau steps, is not distinguishable from the plateau age (Fig. 4g). The radiogenic ^{40}Ar of these ten steps are lower than 12%, thus these data are clustered near the y-axis and the $^{39}Ar/^{40}Ar$ intercept value has a large error. In this case, we regard the plateau age 21.0 ± 2.5 Ma as a reasonable estimate for the age of lava SW8-8.

4.2. The Shanwang Formation

Sample SW01 gives a strongly discordant age spectrum (Fig. 5a), yet a large percentage of the gas (80%, six consecutive steps) suggests a near plateau age of about 17 Ma. These six steps yield an inverse isochron age of about 17 Ma (Fig. 5b). We regard 17 Ma as approximation for the time since lava SW01 erupted.

Sample SW2007 belongs to the same lava flow as sample SW01, and also gives a discordant age spectrum (Fig. 5c). Steps 4–7, which account for 61.4% of the total ^{39}Ar released, suggest a near plateau age of 18 Ma. These four steps yield an inverse isochron age of about 18 Ma (Fig. 5d).

4.3. The Yaoshan Formation

Sample SW8-13 gives a nearly concordant age spectrum (Fig. 6a). Twelve consecutive steps which account for 98.8% of the total ^{39}Ar released, define a plateau age of 18.0 ± 0.8 Ma (MSWD = 0.7). An inverse isochron age of 17.3 ± 1.5 Ma (MSWD = 0.7) (Fig. 6b), calculated from these plateau steps, is not distinguishable from the plateau age. The $^{40}Ar/^{36}Ar$ intercept of 297.6 ± 4.2 is in good agreement with the air ratio. The concordant age spectra and the atmospheric $^{40}Ar/^{36}Ar$ intercept value indicate that there is no resolvable excess argon contamination. Because no assumptions are made about the initial $^{40}Ar/^{36}Ar$ ratio or its uncertainty, we interpret the isochron age 17.3 ± 1.5 Ma as a reasonable estimate for the time since eruption of lava SW8-13.

5. Discussion and conclusions

5.1. Previous geochronological and paleomagnetic studies of the Shanwang sequence

Since the early 1980s many studies have attempted to use K–Ar and Ar–Ar dating to constrain the age of the Shanwang Formation and associated Shanwang biota (summarized in Table 2). The age estimates of the inter-bedded basalt in the Shanwang Formation range from 10 to 29 Ma; the age of the basalt in the underlying Niushan Formation ranges from 12 to 44 Ma, while the age of the basalt in the overlying Yaoshan Formation ranges from 8 to 21 Ma (also see Table 2 and references therein). These widely scattered age estimates may reflect alteration and/or excess argon in basalts.

Paleomagnetic study of the Shanwang sequence was first conducted by Fang et al. (1980) and Ye and Yuan (1980). Fang et al. (1980) collected 19 oriented paleomagnetic samples from the bas-

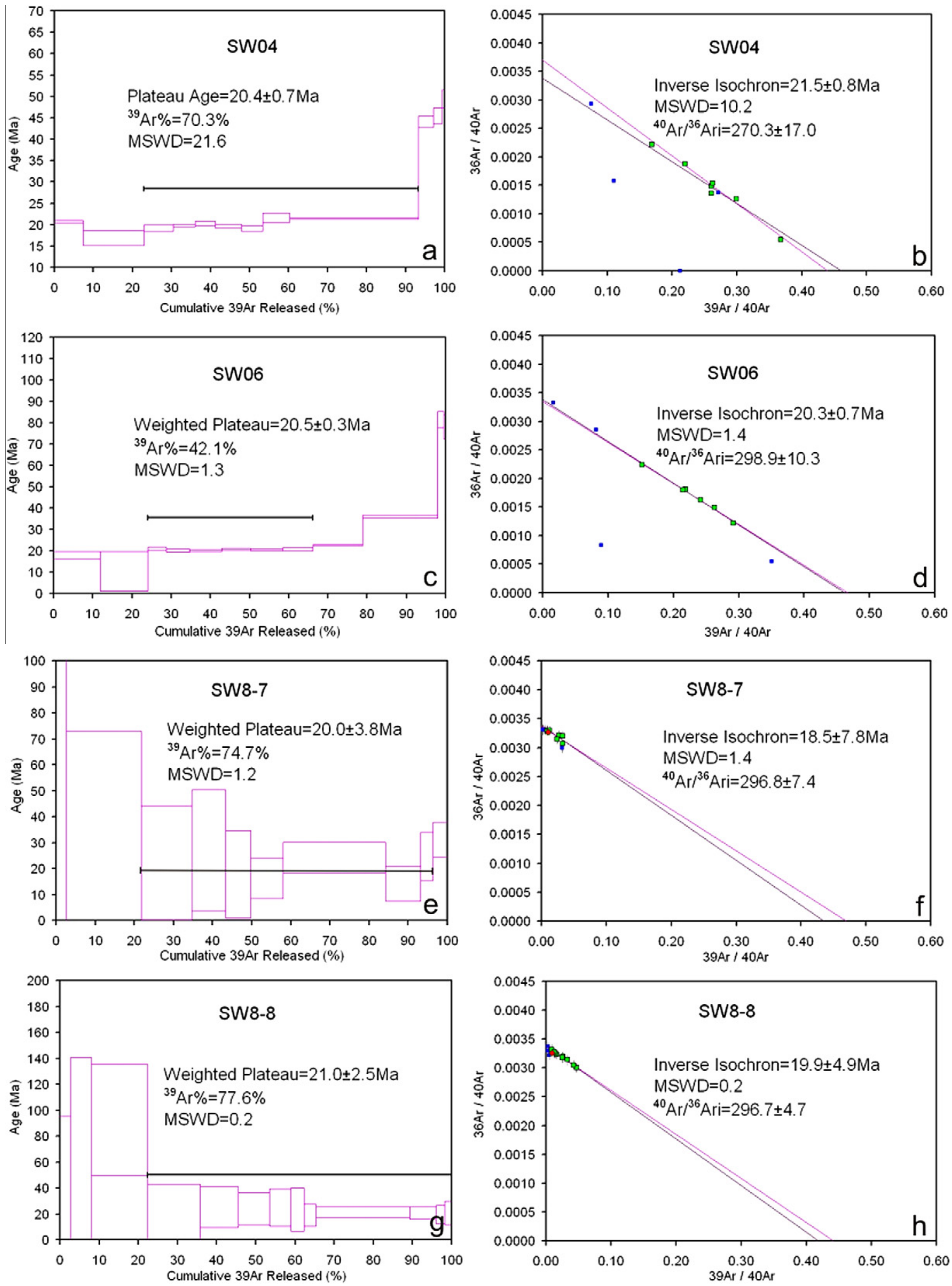

Fig. 4. Age spectra and inverse isochron correlation diagrams for samples from the Niushan Formation.

alts of the Shanwang Basin: eight from the Niushan Formation, four from the Shanwang Formation, and seven from the Yaoshan Formation. Only natural remanent magnetizations (NRMs) of the samples were measured using a LAM-24 astatic magnetometer, leading the authors recognized five magnetozones: two in the Niushan Formation (the lower one N1 being normal; and the upper one R1, reverse), two in the Shanwang Formation (the lower one N2 being normal; and the upper one R2, reverse), and one normal N3 in the Yaoshan Formation. Considering a K–Ar age of ∼21 Ma for the basalt from magnetozone R2 of the Shanwang Formation, Fang

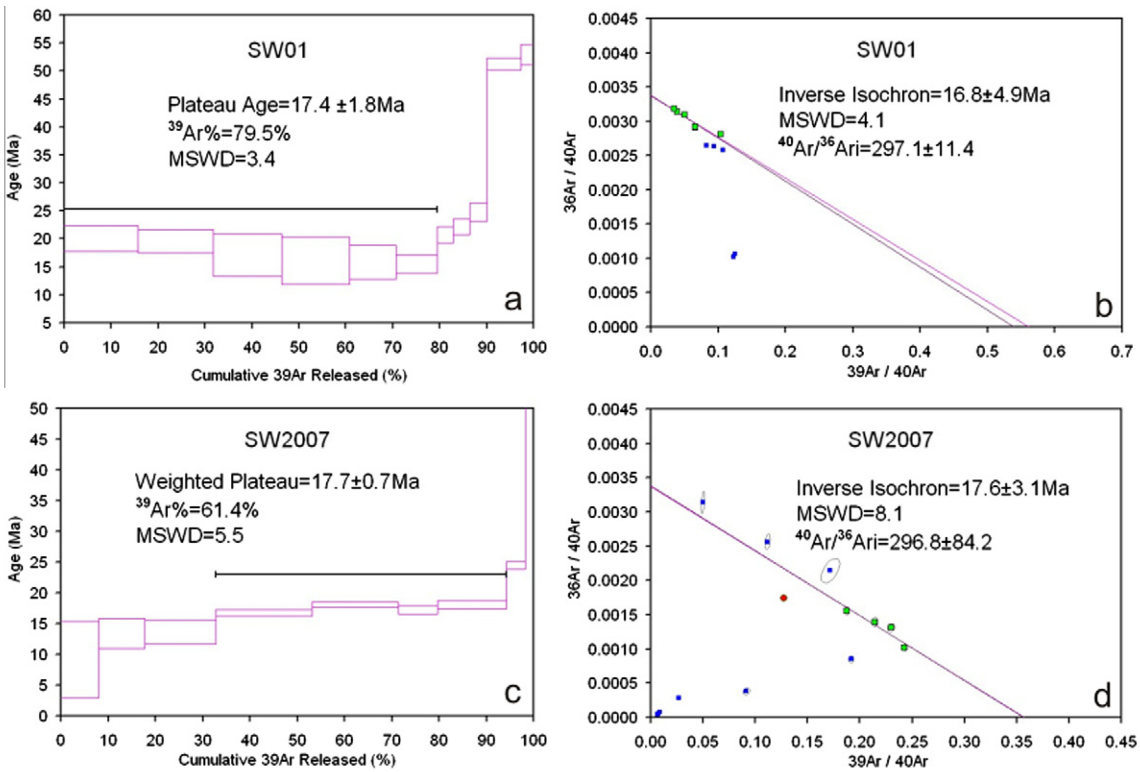

Fig. 5. Age spectra and inverse isochron correlation diagrams for samples from the Shanwang Formation.

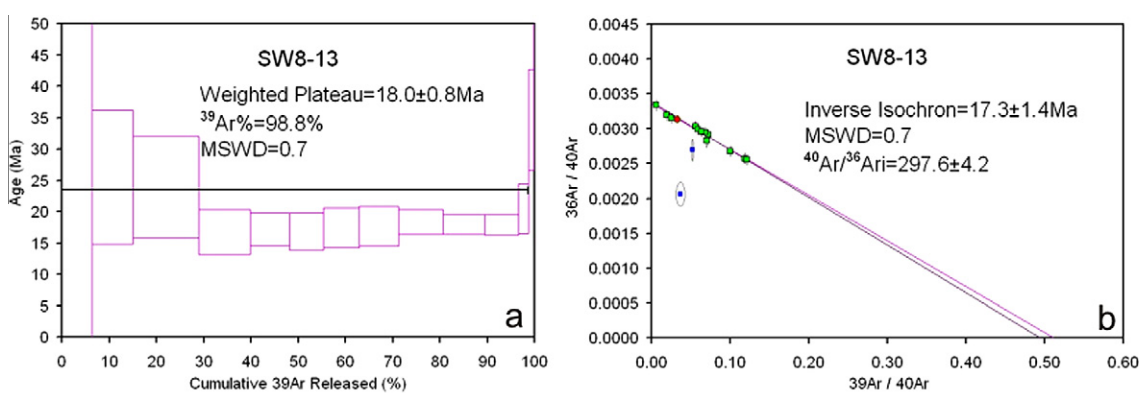

Fig. 6. Age spectra and inverse isochron correlation diagrams for samples from the Yaoshan Formation.

et al. (1980) proposed that the basalts in the Shanwang Basin erupted during the period of 27–17 Ma based on the geomagnetic polarity time scale developed by Heirtzler et al. (1968).

Subsequently, Ye and Yuan (1980) collected six oriented paleomagnetic samples from the diatomaceous sediments of the Shanwang Formation. The samples were subjected to stepwise AF demagnetization up to 10 mT; remanences were measured using a LAM-24 astatic magnetometer. These authors found that all the diatomaceous samples are of normal polarity.

Nearly 10 years later, Liu and Shi (1989) collected 16 oriented paleomagnetic samples from the diatomaceous sediments of the Shanwang Formation. The samples were subjected to stepwise thermal demagnetization up to 260 °C using a Schonstedt thermal demagnetizer. A secondary magnetic component, probably of viscous origin, was present and was removed by thermal demagnetization at 100–150 °C. Remanences were measured using a GM401A superconducting magnetometer. These authors found that all the diatomaceous samples are of normal polarity, well consistent with the results of Ye and Yuan (1980).

Given the widely scattered radiometric age estimates and preliminary paleomagnetic investigations in earlier studies, it is doubtful that those results could have provided stringent constraints on the age of the Shanwang Formation and associated biota.

5.2. Age of the basalts in the Niushan Formation

Previous K–Ar age estimates for the basalts from the Niushan Formation range from 12 to 44 Ma, but concentrate between 16 and 18 Ma (Table 2). Sample SW04 and SW06 yield discordant age spectrum, sample SW04 and SW06 yield discordant age spectrum, giving older ages at high temperature steps (1100–1450 °C) that follow the near plateau. The ratio of $^{37}Ar/^{39}Ar$ showed a distinct increase at older ages steps (Table 1), indicating the degas of calcium rich phase (pyroxene or olivine), thus the age of low temperature steps that formed the near plateau might not have been heavily contaminated by excess argon in xenocrystals. This presumption is confirmed by the near plateau ages (20–21 Ma) that are overlapped by 'good plateau ages' of sample SW8-8.

Table 2
Age of Cenozoic basalt in the Shanwang Basin.

Formation	Age (Ma)	Method	Sample ID	Locality	References
Yaoshan	7.86 ± 0.5	K–Ar	Ch-6	Top of Jiaoyanshan	Wang et al. (1981)
Yaoshan	13.5 ± 0.5	K–Ar	Ch-1	Top of Niushan	Wang et al. (1981)
Yaoshan	10.64 ± 0.28	K–Ar	SLJ-65	Yaoshan	Chen and Peng (1985)
Yaoshan	11.40 ± 0.31	K–Ar	SLJ-68	Yaoshan	Chen and Peng (1985)
Yaoshan	13.85 ± 0.37	K–Ar	SLJ-72	Yaoshan	Chen and Peng (1985)
Yaoshan	13.59 ± 0.37	K–Ar	SLJ-72	Yaoshan	Chen and Peng (1985)
Yaoshan	15.77 ± 0.44	K–Ar	SLJ-51	Jushan	Chen and Peng (1985)
Yaoshan	13.43 ± 0.36	K–Ar	SLJ-54	Jushan	Chen and Peng (1985)
Yaoshan	10–12 Ma, apparent ages	K–Ar	ss008, s009, ss011, ss032, ss033	Base of Yaoshan, overlied on the coal layer	Zhu et al. (1985)
Yaoshan	11–18 Ma, apparent ages	K–Ar	ss012, s013, ss014, ss016, ss018	Upper part of Yaoshan	Zhu et al. (1985)
Yaoshan	15–21 Ma, apparent ages	K–Ar	ss019, s020, ss021	Upper part of Xiaoyaoshan	Zhu et al. (1985)
Shanwang	22.5 ± 1.9	K–Ar	Ch-9	Top of Yaoshan	Wang et al. (1981)
Shanwang	23.0 ± 1.6	K–Ar	Ch-9	Top of Yaoshan	Wang et al. (1981)
Shanwang	20.0 ± 2	K–Ar	Ch-10	Middle of Yaoshan	Wang et al. (1981)
Shanwang	24.0 ± 1.2	K–Ar	Ch-5	Middle of Jiaoyanshan	Wang et al. (1981)
Shanwang	15.23 ± 0.17	K–Ar		Basalts layered with sediments in Shanwang	Zhao et al. (2002)
Shanwang	9.83 ± 0.22	K–Ar		Basalts layered with sediments in Shanwang	Zhao et al. (2002)
Shanwang	13.28–14.41	Ar–Ar		The lower temperature plateau of above samples	Zhao et al. (2002)
Shanwang	About 29	Ar–Ar		The higher temperature plateau of above samples	Zhao et al. (2002)
Niushan	44.1 ± 4	K–Ar	Ch-7	Base of Jiaoyanshan	Wang et al. (1981)
Niushan	44.0 ± 2	K–Ar	Ch-8	Base of Yaoshan	Wang et al. (1981)
Niushan	16.05 ± 0.43	K–Ar	SLJ-42	Niushan	Chen and Peng (1985)
Niushan	16.19 ± 0.42	K–Ar	SLJ-48	Niushan	Chen and Peng (1985)
Niushan	18.05 ± 0.55	K–Ar	SEALPH	Base of Jiaoyanshan, overlied by diatom sediments	Chen and Peng (1985)
Niushan	16.06 ± 0.42	K–Ar	Lj-42	Niushan	Jin (1985)
Niushan	16.19 ± 0.42	K–Ar	Lj-42	Niushan	Jin (1985)
Niushan	18.87 ± 0.49	K–Ar	Lj-48	Niushan	Jin (1985)
Niushan	12–15	K–Ar	ss002, ss003, ss004, ss005, ss006, ss007	Base of Jiaoyanshan	Zhu et al. (1985)

Although sample SW8-7 yields a discordant age spectrum with very large error bar due to its low K content and vesicular texture, the near plateau age of 20 Ma also agrees well with 21.0 ± 2.5 Ma of sample SW8-8. Thus we interpret 21.0 ± 2.5 Ma as the eruption age of the Niushan Formation basalt.

5.3. Age of the basalts in the Shanwang Formation

Previous K–Ar age estimates for basalts from the Shanwang Formation range from 10 to 29 Ma (Table 2). Three samples were measured by $^{40}Ar/^{39}Ar$ step heating. Unfortunately, all spectra show two plateau ages (Zhao et al., 2002). Zhao et al. (2002) believe the higher temperature plateau ages (29.00 ± 0.07 to 29.37 ± 0.10 Ma) may be contaminated by excess argon in xenocrystals, and assume the lower extraction temperature plateau age 13.28 ± 0.14 to 14.41 ± 0.07 Ma as the eruption age of basalts interbedded in the Shanwang Formation.

Samples SW2007 and SW01 were collected from the basalt just below the diatomaceous sediments of the Shanwang Formation. The age spectrum of sample SW2007 and SW01 are discordant, giving older ages at high temperature steps (1100–1450 °C) that follow the near plateau. The ratio of $^{37}Ar/^{39}Ar$ showed a distinct increase at older ages steps (Table 1), indicating degas of calcium rich phase (pyroxene or olivine). Thus the near plateau ages (17–18 Ma) may be contaminated by excess argon in xenocrystals and may be older than eruption age. Lava SW8-13 from Yaoshan Formation is capping on SW2007 and SW01 and should be younger. However, its concordant isochron age (17.3 ± 1.5 Ma) agree well with the near plateau ages (17–18 Ma) of SW2007 and SW01, suggest that the age of low temperature steps that formed the near plateau might not have been heavily contaminated by excess argon in xenocrystals. Therefore, the eruption age of the basalt just below the fossiliferous layer in the Shanwang Formation is estimated to be about 17 Ma.

5.4. Age of the basalts in the Yaoshan Formation

Because pollen and vertebrate fossils found in the fluvial conglomerates are similar to those collected in the Shanwang Formation, some researchers consider the contact with the overlying Yaoshan Formation to be conformable. This suggests the age of the two formations may be very close (Yan et al., 1983). However, previous K–Ar ages estimates for the basalts in the Yaoshan Formation range from 8 to 21 Ma, and concentrate about 10 Ma (Table 2). Sample SW8-13, which was taken from a lava flow on the slope of the Yaoshan Hill, overlying Yaoshan conglomerates, yields an age of 17.3 ± 1.4 Ma (Fig. 6). Thus we propose that the basalts in the Yaoshan Formation erupted around 17 Ma.

5.5. Age of the Shanwang biota and its implication

The age of the Shanwang biota is constrained by the age of the basalt just below the fossil-bearing diatomaceous sediments of the Shanwang Formation and the age of the basalt of the overlying Yaoshan Formation. Samples SW2007 and SW01 from the basalt just below the fossil-bearing diatomaceous sediments of the Shanwang Formation yield near plateau age of 17–18 Ma. Sample SW8-13 from a lava flow in the Yaoshan Formation yields an age of 17.3 ± 1.4 Ma (Fig. 6b). These age determinations suggest that, the age of the Shanwang biota is ca. 17 Ma, which is late Burdigalian Age of the Early Miocene in the widely-used Geologic Time Scale 2004 (Gradstein et al., 2004).

Previous correlations of the Shanwang fauna with the well-calibrated European and North American Land Mammal Ages have varied due to the poor age constraints. It has been correlated with MN6 (Yan et al., 1983), MN3-5 (Li et al., 1984), MN5 (Qiu and Qiu, 1995; Qiu et al., 1999), and MN4 (Deng et al., 2003; Deng, 2006). The age of 17 Ma presented in this study of the Shanwang biota supports previous interpretations that this mammal fauna can be correlated with MN4 in the middle Orleanian of the European Land Mammal Age (Steininger et al., 1996; Steininger, 1999; Agustí et al., 2001), the late Hemingfordian of the North American Land Mammal Age (Woodburne and Swisher, 1995; Alroy, 2000), and the Santacrucian of the South American Land Mammal Ages (Flynn and Swisher, 1995). This more precise age and the resultant correlation with other deposits worldwide contributes to the establishment of the chronological sequence of Chinese Neogene mammalian faunas, and gives further insight into the study of mammalian terrestrial evolution and the intercontinental dispersal of different clades.

Furthermore, the age control of the Shanwang Formation enables us to discuss the linkage between biological diversity and paleoenvironment. The new age estimate indicates that the Shanwang biota coincides with the onset of the mid-Miocene Climate Optimum (17–15 Ma) (Zachos et al., 2001), which marks the warmest and the most humid period of the Miocene. This episode is also a critical period for biotic turnover (Blois and Hadly, 2009). The Shanwang fauna consists mainly of mammals that prefer warm and moist habitats (Qiu and Li, 2005), and the Shanwang flora indicates a forest landscape with a humid and warm temperate to subtropical climate (Sun et al., 2002; Sun and Wang, 2005; Strömberg et al., 2007). Moreover, the sedimentary facies of the Shanwang Formation suggests a lake environment. All these lines of evidence imply much warmer and more humid climate compared with the present local sub-humid temperate environment. These characteristics of the faunal and floral components are consistent with paleoenvironmental reconstructions that suggest eastern China, including the Shanwang Basin, was dominated by humid climates during this period (Yang et al., 2007; Guo et al., 2008). Actually, this optimal climate not only occurred in eastern China but also in the inland basins of northwestern China (Sun and Zhang, 2008). Additionally, worldwide pollen records reveal a mid-Miocene subtropical to warm-temperate humid climate in Europe (e.g., Utescher et al., 2000; Jiménez-Morenoa et al., 2005; Jiménez-Moreno and Suc, 2007) and warm conditions in East Antarctica (Hannah, 2006). The constraints on the age of the Shanwang Biota presented here yield new perspectives on the dynamics of plant and mammalian ecosystems during the onset of the Middle Miocene Climatic Optimum. In this sense, the biological diversity of the Shanwang Formation is a response to the global-scale mid-Miocene Climatic Optimum.

Acknowledgments

The authors thank Dr. Jingmai O'Connor for her language corrections, which have significantly improved the manuscript. We also thank Mr. Gang Zhao, Mr. Junde Li and Mr. Chunke Li for their help in the field. All the measurements were made at the Paleomagnetism and Geochronology Laboratory (SKL-LE), Institute of Geology and Geophysics, Chinese Academy of Sciences. This work is supported by China MOST 973 Program (grant 2009CB825001), the National Natural Science Foundation of China (grants 90714010, and 40821091), Chinese Academy of Sciences (grants KZCX2-YW-Q08-2-2 and KZCX2-YW-JS101). CD acknowledges further support from the National Natural Science Foundation of China grant 40925012 and the Chinese Academy of Sciences grant KZCX2-EW-117.

References

Agustí, J., Cabrera, L., Garcés, M., Krijgsman, W., Oms, O., Parés, J.M., 2001. A calibrated mammal scale for the Neogene of Western Europe. State of the art. Earth-Science Reviews 52 (4), 247–260.

Alroy, J., 2000. New methods for quantifying macroevolutionary patterns and processes. Paleobiology 26 (4), 707–733.

Blois, J.L., Hadly, E.A., 2009. Mammalian response to Cenozoic climatic change. Annual Review of Earth and Planetary Sciences 37, 181–208.

Chen, D.G., Peng, Z.C., 1985. K–Ar ages and Pb, Sr isotopic characteristics of Cenozoic volcanic rocks in Shandong, China. Geochemica 4, 303–311.

Deng, T., 2006. Chinese Neogene mammal biochronology. Vertebrata PalAsiatica 44, 143–163.

Deng, T., Wang, W.M., Yue, L.P., 2003. Recent advances of the establishment of the Shanwang Stage in the Chinese Neogene (in Chinese with English abstract). Vertebrata PalAsiatica 41, 314–323.

Fang, D.J., Zhu, X.Y., He, L.Z., Lu, Y.S., 1980. The study of palaeomagnetism in Cainozoic basalts and its strata meaning at San-huang District, Santung (in Chinese with English abstract). Journal of Chekiang University S1, 49–57.

Flynn, J.J., Swisher III, C.C., 1995. Cenozoic South American land mammalian ages: correlation to global geochronologies. In: Berggren, W.A., Kent, D.V., Auby, M.-P., Hardenbol, J. (Eds.), Geochronology Time Scales and Global Stratigraphic Correlation. SEPM Special Publication No. 54, pp. 317–333.

Gradstein, F.M., Ogg, J.G., Smith, A.G., 2004. A Geologic Time Scale 2004. Cambridge University Press, Cambridge (UK), pp. 589.

Guo, Z.F., Liu, J.Q., Chen, X.Y., 2007. Effect of Miocene basaltic volcanism in Shanwang (Shandong Province, China) on environmental changes. Science in China Series D: Earth Sciences 50 (12), 1823–1827.

Guo, Z.T., Sun, B., Zhang, Z.S., Peng, S.Z., Xiao, G.Q., Ge, J.Y., Hao, Q.Z., Qiao, Y.S., Liang, M.Y., Liu, J.F., Yin, Q.Z., Wei, J.J., 2008. A major reorganization of Asian climate by the early Miocene. Climate of the Past 4 (3), 153–174.

Hannah, M.J., 2006. The palynology of ODP site 1165, Prydz Bay, East Antarctica: a record of Miocene glacial advance and retreat. Palaeogeography, Palaeoclimatology, Palaeoecology 231, 120–133.

He, H.Y., Wang, X.L., Zhou, Z.H., Wang, F., Boven, A., Shi, G.H., Zhu, R.X., 2004. Timing of the Jiufotang Formation (Jehol Group) in Liaoning, northeastern China and its implications. Geophysical Research Letters 31 (12), L12605, doi:10.1029/2004GL019790.

Heirtzler, J.R., Dickson, G.O., Herron, E.M., Pittman III, W.C., Le Pichon, X., 1968. Marine magnetic anomalies, geomagnetic field reversals, and motions of the ocean floor and continents. Journal of Geophysical Research 73, 2119–2136.

Jiménez-Moreno, G., Suc, J.P., 2007. Middle Miocene latitudinal climatic gradient in Western Europe: evidence from pollen records. Palaeogeography, Palaeoclimatology, Palaeoecology 253, 208–225.

Jiménez-Morenoa, G., Rodríguez-Tovara, F.J., Pardo-Igúzquizac, U., Fauquetted, S., Suc, J.P., Müller, P., 2005. High-resolution palynological analysis in late early–middle Miocene core from the Pannonian Basin, Hungary: climatic changes, astronomical forcing and eustatic fluctuations in the Central Paratethys. Palaeogeography, Palaeoclimatology, Palaeoecology 216, 73–97.

Jin, L.Y., 1985. K–Ar ages of Cenozoic volcanic rocks in the middle segment of the Tancheng-Lujiang fault zone and stages of related volcanic activity. Geological Review 31, 309–315.

Koppers, A.A.P., 2002. ArArCALC – software for $^{40}Ar/^{39}Ar$ age calculations. Computers & Geosciences 28, 605–619.

Li, F.L., 1991. Reconsideration of the Shanwang Formation, Linqu, Shandong (in English with English abstract). Journal of Stratigraphy 15 (2), 123–129.

Li, C.K., Wu, W.Y., Qiu, Z.D., 1984. Chinese Neogene: subdivision and correlation (in Chinese with English abstract). Vertebrata PalAsiatica 22, 163–178.

Li, Y.-M., Ferguson, D.K., Wang, Y.-F., Li, C.-S., 2010. Paleoenvironmental inferences from diatom assemblages of the middle Miocene Shanwang Formation, Shandong, China. Journal of Paleolimnology 43 (4), 799–814.

Liang, M.M., Bruch, A., Collinson, M., Mosbrugger, V., Li, C.S., Sun, Q.G., Hilton, J., 2003. Testing the climatic estimates from different palaeobotanical methods: an example from the Middle Miocene Shanwang flora of China. Palaeogeography, Palaeoclimatology, Palaeoecology 198, 279–301.

Liu, L.P., Fortelius, M., Pickford, M., 2002. New fossil Suidae from Shanwang, Shandong, China. Journal of Vertebrate Paleontology 22 (1), 152–163.

Liu, H.F., Shi, N., 1989. Paleomagnetic study of Shanwang Formation, Shandong Province (in Chinese with English abstract). Acta Scientiarum Naturalium – Universitatis Pekinensis 25 (5), 585–593.

Luo, Z.H., Li, F.L., Yang, M.H., 1992. On origin of the Shanwang Basin and its geological significance. Geoscience: Journal of Graduate School, China University of Geosciences 6 (1), 30–38.

Ogg, J.G., Ogg, G., Gradstein, F.M., 2008. The Concise Geologic Time Scale. Cambridge University Press, Cambridge (UK).

Qiu, Z.D., Li, C.K., 2005. Evolution of Chinese mammalian faunal regions and elevation of the Qinghai-Xizang (Tibet) Plateau. Science in China, Series D-Earth Sciences 48 (8), 1246–1258.

Qiu, Z.X., Qiu, Z.D., 1995. Chronological sequence and subdivision of Chinese Neogene mammalian faunas. Palaeogeography, Palaeoclimatology, Palaeoecology 116, 41–70.

Qiu, Z.X., Wu, W.Y., Qiu, Z.D., 1999. Miocene mammal faunal sequence of China: palaeozoogeography and Eurasian relationships. In: Rössner, G.E., Heissig, K. (Eds.), The Miocene Land Mammals of Europe. Verlag Dr. Friedrich Pfeil, München, pp. 443–455.

Renne, P.R., Swisher, C.C., Deino, A.L., Karner, D.B., Owens, T.L., DePaolo, D.J., 1998. Intercalibration of standards, absolute ages and uncertainties in $^{40}Ar/^{39}Ar$ dating. Chemical Geology 145, 117–152.

Skvortzov, B.V., 1937. Neogene diatoms from eastern Shantung. Bulletin of the Geological Society of China 17 (2), 193–208.

SPBGMR (Shandong Provincial Bureau of Geology and Mineral Resources), 1991. Regional Geology of Shandong Province. Geological Press, Beijing.

Steiger, R.H., Jaeger, E., 1977. Subcommission on geochronology: convention on the use of decay constants in geo- and cosmochronology. Earth and Planetary Science Letters 36, 359–362.
Steininger, F.F., 1999. Chronostratigraphy, Geochronology and Biochronology of the Miocene "European Land Mammal Mega-Zones" (ELMMZ) and the Miocene "Mammal Zones (MN-Zones)". In: Gertrud, E., Rössner, Heissig, K. (Eds.), The Miocene Land Mammals of Europe. Verlag Dr. Friedrich Pfeil, München, pp. 9–24.
Steininger, F.F., Berggren, W.A., Kent, D.V., Bernor, R.L., Sen, S., Agusti, J., 1996. Circum-Mediterranean Neogene (Miocene and Pliocene) marine-continental chronologic correlations of European mammal units. In: Bernor, R.L., Fahlbusch, V., Mittmann, H.W. (Eds.), The Evolution of Western Eurasian Neogene Mammal Faunas. Columbia University Press, New York., pp. 7–44.
Strömberg, C.A.E., Friis, E.M., Liang, M.M., Werdelin, L., Zhang, Y.L., 2007. Palaeoecology of an early-middle Miocene lake in China: preliminary investigations based on phytoliths from the Shanwang Basin. Vertebrata PalAsiatica 45, 145–160.
Sun, A.L., 1961. Notes on fossil snakes from Shanwang, Shantung (in Chinese with English abstract). Vertebrata PalAsiatica 5, 306–312.
Sun, Q.G., Collinson, M.E., Li, C.S., Wang, Y.F., Beerling, D.J., 2002. Quantitative reconstruction of palaeoclimate from the Middle Miocene Shanwang flora, eastern China. Palaeogeography, Palaeoclimatology, Palaeoecology 180, 315–329.
Sun, X.J., Wang, P.X., 2005. How old is the Asian monsoon system? – Palaeobotanical records from China. Palaeogeography, Palaeoclimatology, Palaeoecology 222, 181–222.
Sun, J.M., Zhang, Z.Q., 2008. Palynological evidence for the Mid-Miocene Climatic Optimum recorded in Cenozoic sediments of the Tianshan Range, northwestern China. Global and Planetary Change 64, 53–68.
Teilhard De Chardin, P., 1939. The Miocene Cervids from Shantung. Bulletin of the Geological Society of China 19 (3), 269–278.
Tong, Y.S., Zheng, S.H., Qiu, Z.D., 1995. Cenozoic mammal ages of China (in Chinese with English abstract). Vertebrata PalAsiatica 33 (4), 290–314.
Utescher, T., Mosbrugger, V., Ashraf, A., 2000. Terrestrial climate evolution in Northwest Germany over the last 25 million years. Palaios 15, 430–449.
Wang, W.W., 2006. Correlation of pollen sequences in the Neogene palynofloristic regions of China. Palaeoworld 15, 77–99.
Wang, H.F., Zhu, B.Q., Fan, C.Y., Dong, L.M., 1981. A study on K–Ar isotopic ages if Cenozoic basalts from Linqu area, Shandong Province. Geochimica 4, 321–328.
Woodburne, M.O., Swisher III, C.C., 1995. Land mammal high-resolution geochronology, intercontinental overland dispersals, sea level, climate, and vicariance. In: Berggren, W.A., Kent, D.V., Aubry, M.-P., Hardenbol, J. (Eds.), Geochronology, Time Scales, and Global Stratigraphic Correlation. SEPM Special Publication No. 54, pp. 335–364.
Xu, J.F., Qiu, J.X., 1991. The fractionalal crystallization of basaltic magma in Shanwang area, Shandong Province (in Chinese with English abstract). Earth Science – Journal of China University of Geosciences 16 (4), 369–376.
Yan, D.F., Qiu, Z.D., Meng, Z.Y., 1983. Miocene stratigraphy and mammals of Shanwang, Shandong (in Chinese with English abstract). Vertebrata PalAsiatica 21, 210–222.
Yang, H., 2000. AAPG Studies in Geology #46, Chapter 43: The Shanwang Basin (Miocene) in Shandong Province. Eastern China. AAPG Special Volumes, Volume Lake Basins Through Space and Time, pp. 473–479.
Yang, H., Yang, S.P., 1994. The Shanwang fossil biota in eastern China: a Miocene *Konservat-Lagerstätte* in lacustrine deposits. Lethaia 27, 345–354.
Yang, J., Wang, Y.F., Spicer, R.A., Mosbrugger, V., Li, C.S., Sun, Q.G., 2007. Climatic reconstruction at the Miocene Shanwang basin, China, using leaf margin analysis, CLAMP, coexistence approach, and overlapping distribution analysis. American Journal of Botany 94 (4), 599–608.
Ye, S.J., Yuan, B.Y., 1980. A paleomagnetic study on diatomaceous earth of Shanwang Formation (Miocene) in Linqu County, Shandong (in Chinese). Acta Geophysica Sinica 23 (4), 459–463.
Young, C.C., 1936. On the Cenozoic geology of Itu, Changlo and Linchü districts (Shantung). Bulletin of the Geological Society of China 15, 171–187.
Young, C.C., 1937. On a Miocene mammalian fauna from Shantung. Bulletin of the Geological Society of China 17, 209–244.
Young, C.C., Tchang, T.L., 1936. Fossil fishes from the Shanwang Series of Shantung. Bulletin of the Geological Society of China 15, 197–205.
Zachos, J., Pagani, M., Sloan, L., Thomas, E., Billups, K., 2001. Trends, rhythms, and aberrations in global climate 65 Ma to present. Science 292, 686–693.
Zhao, R., Han, B., Liou, J.G., 2002. Timing of Basalt Flows in the Shanwang Basin, Shandong Peninsula, Eastern China. Eos Trans. AGU, 83(47), Fall Meeting Supplement, Abstract V62B-1406.
Zhu, M., Hu, H.G., Zhao, D.Z., Liu, S.L., Hu, X.Z., Ma, Z.Q., Jian, W.Y., 1985. Potassium–Argon dating of Neogene basalt in Shanwang area, Shandong Province. Petrological Research 5, 47–59.